INTERNATIONAL JOURNAL FOR NUMERICAL METHODS IN ENGINEERING
Int. J. Numer. Meth. Engng 2006; **65**:2007–2034
Published online 14 November 2005 in Wiley InterScience (www.interscience.wiley.com). DOI: 10.1002/nme.1486

The simple boundary element method for multiple cracks in functionally graded media governed by potential theory: a three-dimensional Galerkin approach

Glaucio H. Paulino*, † and Alok Sutradhar

Department of Civil and Environmental Engineering, University of Illinois at Urbana-Champaign, Newmark Laboratory, 205 North Mathews Avenue, Urbana, IL 61801, U.S.A.

SUMMARY

The simple boundary element method consists of recycling existing codes for homogeneous media to solve problems in non-homogeneous media while maintaining a purely boundary-only formulation. Within this scope, this paper presents a 'simple' Galerkin boundary element method for multiple cracks in problems governed by potential theory in functionally graded media. Steady-state heat conduction is investigated for thermal conductivity varying either parabolically, exponentially, or trigonometrically in one or more co-ordinates. A three-dimensional implementation which merges the dual boundary integral equation technique with the Galerkin approach is presented. Special emphasis is given to the treatment of crack surfaces and boundary conditions. The test examples simulated with the present method are verified with finite element results using graded finite elements. The numerical examples demonstrate the accuracy and efficiency of the present method especially when multiple interacting cracks are involved. Copyright © 2005 John Wiley & Sons, Ltd.

KEY WORDS: cracks; boundary element method; Galerkin; functionally graded materials; non-homogeneous media; three-dimensional analysis; potential theory

1. INTRODUCTION

Fracture geometries arise in important engineering applications governed by potential theory. Modelling of subsurface flow often deal with fractures in the rock [1–3] or soil systems having embedded thin layers of different permeability [4]. Simulation of an electroplating process provides an important industrial application [5, 6]. Moving boundary problems, such as crack

*Correspondence to: Glaucio H. Paulino, Department of Civil and Environmental Engineering, University of Illinois at Urbana-Champaign, Newmark Laboratory, 205 North Mathews Avenue, Urbana, IL 61801, U.S.A.
†E-mail: paulino@uiuc.edu

Contract/grant sponsor: NSF; contract/grant number: CMS-0115954
Contract/grant sponsor: Computational Science and Engineering Program (CSE, UIUC)

Received 7 January 2005
Revised 18 April 2005
Accepted 20 July 2005

Copyright © 2005 John Wiley & Sons, Ltd.

propagation, is an area in which the boundary element method (BEM) is best suited. Remeshing an evolving geometry for crack propagation problems is much simpler with boundary element analysis than with a domain-based analysis such as the finite element method (FEM), especially if multiple interacting cracks are involved.

In this paper, crack problems governed by potential theory in functionally graded media are investigated. In general, a functionally graded material is a special type of composite in which the constituent volume fraction varies gradually leading to a non-uniform microstructure with continuously graded macroproperties, e.g. thermal conductivity, density and specific heat. For instance, for problems governed by potential theory, e.g. steady-state heat transfer, the thermal conductivity is a function of position, i.e. $k \equiv k(\mathbf{x})$. Basic literature regarding functionally graded materials (FGMs), can be found in the books by Suresh and Mortensen [7] and Miyamoto *et al.* [8], in the special issue of the Materials Science and Engineering journal which contains papers from the German Priority Programme (FGMs) [9], and in the review chapter by Paulino *et al.* [10].

In recent years, the Galerkin BEM (GBEM) has emerged as a powerful numerical method in computational mechanics [11]. To solve crack problems by the collocation BEM, higher order interpolation using Hermite element or Overhauser element, which possesses C^1 smoothness, is required [12]. For three-dimensional implementations, such higher order elements involve tremendous complexity. An alternative approach consists of using non-conforming elements. Unlike collocation, the Galerkin formulation does not require C^1 interpolation. The Galerkin formulation involves an additional integration over the boundary, that balances out the extra derivative in the hypersingular equation, and thus a C^0 interpolation suffices [13]. Moreover, this technique allows a natural treatment of corners [14] as discussed later. This paper describes an efficient BEM for crack geometries in non-homogeneous media which merges the dual boundary integral equation approach with the Galerkin approximation.

In the BEM literature, most implementations in non-homogeneous media have been developed for non-crack problems. Approaches to treat problems of potential theory in non-homogeneous media include the following:

- Green's function [15, 16].
- Domain integral evaluation [17–25].
- Variable transformation [26, 27].

In the context of BEM, problems of potential theory in non-homogeneous media have been previously studied by Cheng [15, 16], Ang *et al.* [28], Shaw and Makris [29], Shaw [30], Harrouni *et al.* [31, 32], Divo and Kassab [33, 34], Bansal and Pindera [35] and recently by Gray *et al.* [36] and Dumont *et al.* [37]. Most of these works are focussed on obtaining the Green's function.

In the *Green's function approach*, the Green's function has to be derived and a boundary-only formulation can be obtained [15, 16]. A drawback of this approach is that each different material variation requires a different fundamental solution, and thus the kernels for the BEM implementation are different from the standard kernels usually employed for homogeneous problems. As a result, each time a new computer code has to be implemented. Moreover, if the treatment of singularity involves analytical integration, then the process becomes much involved [38]. Several approaches have been developed to evaluate *domain integrals* associated with boundary element formulations including approximate particular solution methods [17, 18], dual reciprocity methods [19], and multiple reciprocity methods [20, 21].

Copyright © 2005 John Wiley & Sons, Ltd.

The particular solution methods and dual reciprocity methods can be considered more or less to be equivalent in nature [25]. These methods have been widely used on the axiom that the domain integral in the boundary integral formulation is somehow removed. In these methods the inhomogeneous term of the governing differential equation is approximated by a simple function such as $(1+r)$ [22] or radial basis functions (RBFs) [23, 39]. The mathematical properties and the convergence rates of the RBF approximations have been studied extensively [23, 24]. In these techniques, the boundary-only nature of the BEM is compromised.

Recently, Sutradhar and Paulino [26] presented a *transformation approach*, called the 'simple BEM', for potential theory problems in non-homogeneous media where non-homogeneous problems are transformed into known problems in homogeneous media. The method leads to a pure boundary-only formulation. This idea has been successfully implemented in three dimensions for steady state [26] and also for transient heat conduction [27] problems where the material property varies in one, two and three dimensions. However, no crack problems were addressed in previous papers. Thus, the present work extends the simple BEM concept for multiple interacting crack problems governed by potential theory.

The remainder of this paper is organized as follows. The simple BEM concept is presented in Section 2. Section 3 describes the fracture algorithm for crack analysis. It isshown that the standard displacement discontinuity approach is not suitable to solve the fracture problem using the 'simple BEM', and thus the dual BEM approach is used to circumvent this situation. Section 4 briefly discusses various aspects of the numerical implementation including treatment of boundary conditions, singularity, and corners. Section 5 demonstrates, by means of numerical examples, that the methodology works and is efficient. Section 6 contains conclusions and final comments.

2. ON THE SIMPLE BEM CONCEPT

The idea of the 'simple BEM' consists of transforming problems in non-homogeneous media to known problems in homogeneous media such that existing codes for homogeneous media can be reused with simple modifications. By means of this approach, which consists of simple changes in the boundary conditions of existing homogeneous heat conduction computer codes, the solutions for non-homogeneous media with quadratic, exponential and trigonometric material variations can be readily obtained.

2.1. Governing equation

For problems described by potential theory, the governing differential equation for a potential function ϕ defined on a region Ω bounded by a surface Γ, with an outward normal $\mathbf{n}$ (see Figure 1), can be written as

$$\nabla \bullet (k(x, y, z)\nabla\phi) = 0 \tag{1}$$

where $k(x, y, z)$ is a position-dependent material function and the dot represents the inner product. Equation (1) is the field equation for a wide range of problems in physics and engineering such as heat transfer, fluid flow motion, flow in porous media, electrostatics and magnetostatics [40]. The boundary conditions of the problem can be of the Dirichlet or Neumann type:

$$\phi = \bar{\phi} \quad \text{on } \Gamma_1 \tag{2}$$

$$q = -k(x, y, z)\frac{\partial\bar{\phi}}{\partial\mathbf{n}} = \bar{q} \quad \text{on } \Gamma_2 \tag{3}$$

Copyright © 2005 John Wiley & Sons, Ltd.

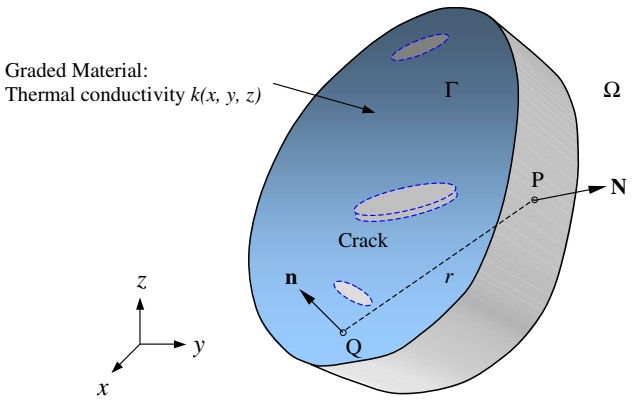

Figure 1. Definition of the boundary value problem with boundary Γ (including crack surfaces and outer boundary) and interior domain Ω.

respectively, with $\Gamma = \Gamma_1 + \Gamma_2$ for a well-posed problem. The boundary value problem is a Dirichlet problem if the potential is known on the whole boundary, whereas it is a Neumann problem if the flux is known on the whole boundary. Mixed boundary conditions are also frequently encountered: flux is prescribed over some portion of the boundary and potential is prescribed over the complementary portion of the boundary [26]. Handling of all those boundary conditions in the context of the 'simple BEM' is described in Section 2.3.

2.2. *Variable transformation approach*

By defining the variable [41]

$$v(x, y, z) = \sqrt{k(x, y, z)}\phi(x, y, z) \tag{4}$$

one rewrites Equation (1) as

$$\nabla^2 v + \left(\frac{\nabla k \bullet \nabla k}{4k^2} - \frac{\nabla^2 k}{2k} \right) v = 0 \tag{5}$$

or, alternatively

$$\nabla^2 v + k'(x, y, z)v = 0 \tag{6}$$

where

$$k' = \frac{\nabla k \bullet \nabla k}{4k^2} - \frac{\nabla^2 k}{2k} \tag{7}$$

By setting $k'(x, y, z) = 0, +\beta^2$ and $-\beta^2$, three classical homogeneous equations namely, the Laplace, standard Helmholtz and the modified Helmholtz can be obtained, respectively. From these cases, a family of variations of $k(x, y, z)$ can be generated, as shown in Table I.

In this paper we focus on variations which depend only on one Cartesian co-ordinate, namely z. From an engineering point of view (for applications such as FGMs), material variation in

Copyright © 2005 John Wiley & Sons, Ltd.

Table I. Family of material variations: transformation approach.

k'	Transformed equation	Material variation	$k(x, y, z)$
0	Laplace: $\nabla^2 v = 0$	Quadratic	$k_0(a_1 + a_2 x)^2(b_1 + b_2 y)^2(c_1 + c_2 z)^2$
β^2	Helmholtz: $\nabla^2 v + \beta^2 v = 0$	Trigonometric	$k_0(a_1 \cos \alpha x + a_2 \sin \alpha x)^2(b_1 \cos \mu y + b_2 \sin \mu y)^2 \times (c_1 \cos \gamma z + c_2 \sin \gamma z)^2$
$-\beta^2$	Modified Helmholtz: $\nabla^2 v - \beta^2 v = 0$	Exponential	$k_0(a_1 e^{\alpha x} + a_2 e^{-\alpha x})^2(b_1 e^{\mu y} + b_2 e^{-\mu y})^2 \times (c_1 e^{\gamma z} + c_2 e^{-\gamma z})^2$

one co-ordinate is of practical importance as described in References [10, 42], which include thermal barrier coatings, bone and dental implants, piezoelectric and thermoelectric devices, graded cementitious materials, and optical application with graded refractive indexes [7–10, 43]. Problems where the material varies in more than one direction have been dealt in References [26, 27].

2.3. Boundary conditions

In order to solve the boundary value problem based on the modified variable v, the boundary conditions of the original problem have to be incorporated in the modified boundary value problem. Thus for the modified problem, the Dirichlet and the Neumann boundary conditions given by Equations (2) and (3) respectively, change as follows:

$$v = \sqrt{k}\,\bar{\phi} \quad \text{on } \Gamma_1 \tag{8}$$

$$\frac{\partial v}{\partial \mathbf{n}} = \frac{1}{2k}\frac{\partial k}{\partial \mathbf{n}} v - \frac{\bar{q}}{\sqrt{k}} \quad \text{on } \Gamma_2 \tag{9}$$

Notice that the Dirichlet boundary condition of the original problem is affected by the factor $\sqrt{k}$. Moreover, the Neumann boundary condition of the original problem changes to a mixed boundary condition (Robin boundary condition). This later modification is the only major change on the boundary value problem.

Another common boundary condition of the original problem is a prescribed relationship between the potential and the flux (e.g. convective heat transfer problems) i.e. Robin type:

$$q = \lambda_1 \phi + \lambda_2 \tag{10}$$

where λ_1 and λ_2 are known constants. The corresponding boundary condition for the modified problem is also a Robin boundary condition, which is given by

$$\frac{\partial v}{\partial \mathbf{n}} = \left(\frac{1}{2k}\frac{\partial k}{\partial \mathbf{n}} - \lambda_1\right) v - \frac{\lambda_2}{\sqrt{k}} \tag{11}$$

Copyright © 2005 John Wiley & Sons, Ltd.

3. CRACK ANALYSIS

Consider a body of arbitrary shape which contains a crack, as shown in Figure 2. The boundary Γ of the body B is composed of non-crack boundary Γ_b and the crack surface Γ_c. The portion of the boundary Γ_b with prescribed potential is denoted by $\Gamma_{b(\phi)}$, and the portion with prescribed flux boundary is denoted by $\Gamma_{b(q)}$. The crack surface Γ_c consists of two coincident surfaces Γ_c^+ and Γ_c^-, representing the upper and lower crack surfaces, respectively. The outward normals to the crack surfaces, designated by n_c^+ and n_c^- are oriented in opposite directions and at any point on the crack surfaces, $n_c^- = -n_c^+$ (see Figure 2). For the non-crack boundaries, standard boundary integral equations (BIE) are written for the Dirichlet portion $\Gamma_{b(\phi)}$, and hypersingular boundary integral equations (HBIE) are written for the Neumann portion $\Gamma_{b(q)}$ (see Figure 2). On the crack surfaces, in order to avoid degeneracy, HBIEs are written on one crack surface and the BIEs are written on the other crack surface. These expressions for a fracture geometry can be written in terms of a 3×3 block matrix. Specifically, the first block row will represent the outer, or non-crack, boundary equations, and the equation for a particular node, as per the usual Galerkin procedure, is chosen according to the prescribed boundary data. In accordance with the dual BEM approach [44, 45], the second and third rows will denote, respectively, the hypersingular and standard equations written on the crack surface. With these definitions, the equations take the abbreviated form

$$\begin{pmatrix} h_{11} & h_{12} & h_{13} \\ h_{21} & h_{22} & h_{23} \\ h_{31} & h_{32} & h_{33} \end{pmatrix} \begin{pmatrix} \Omega_1 \\ V_2 \\ V_3 \end{pmatrix} = \begin{pmatrix} g_{11} & g_{12} & g_{13} \\ g_{21} & g_{22} & g_{23} \\ g_{31} & g_{32} & g_{33} \end{pmatrix} \begin{pmatrix} \hat{\Omega}_1 \\ V_2^{\mathbf{n}} \\ V_3^{\mathbf{n}} \end{pmatrix} \tag{12}$$

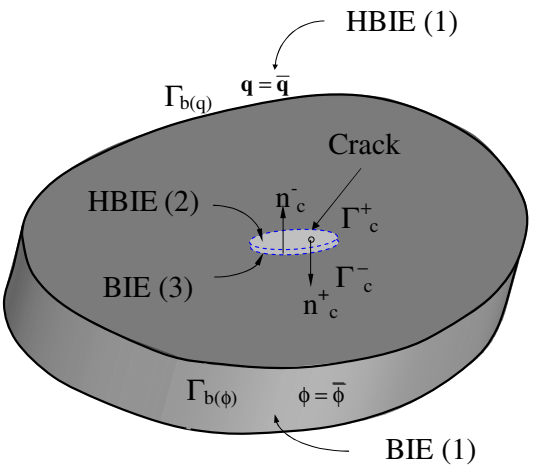

Figure 2. Fracture scheme using the dual BEM approach.

Copyright © 2005 John Wiley & Sons, Ltd.

The vector of unknowns on the non-crack boundary can be a mixture of potential and flux, and is therefore denoted by Ω_1. The corresponding vector of prescribed boundary values is indicated by $\hat{\Omega}_1$. On the fracture, V represents the vector of unknown potential values, $V^{\mathbf{n}}$ the specified flux, and the subscripts $\{2, 3\}$ label the two sides of the crack. The matrix $\mathbf{h}$ on the left therefore multiplies the vector of unknowns, and the right-hand side consists of known quantities.

3.1. Displacement discontinuity approach

The displacement discontinuity approach has been extensively used to solve fracture problems [46, 47]. Notice that, the only difference between the two coincident crack surfaces is the orientation of the normals ($n_c^- = -n_c^+$) and, as a result, $h_{13} = -h_{12}$ and $h_{23} = -h_{22}$. These relationships between the second and third columns are a consequence of the integration over the two sides of the fracture differing by a sign. The usual boundary condition is the derivative quantity (e.g. flux, traction) and thus only the hypersingular equation should be employed.

$$\left(\begin{array}{cc|c} h_{11} & h_{12} & -h_{12} \\ h_{21} & h_{22} & -h_{22} \\ \hline h_{31} & h_{32} & -h_{32} \end{array}\right)\left(\begin{array}{c} \Omega_1 \\ V_2 \\ \hline V_3 \end{array}\right) = \left(\begin{array}{cc|c} g_{11} & g_{12} & g_{12} \\ g_{21} & g_{22} & g_{22} \\ \hline g_{31} & g_{32} & g_{32} \end{array}\right)\left(\begin{array}{c} \hat{\Omega}_1 \\ V_2^{\mathbf{n}} \\ \hline V_3^{\mathbf{n}} \end{array}\right) \tag{13}$$

It is convenient to replace the potential V_2 and V_3 by a single jump in potential

$$\Delta V = V_2 - V_3$$

Similarly on the right-hand side the flux $V_2^{\mathbf{n}}$ and $V_3^{\mathbf{n}}$ is replaced by the flux summation

$$\Sigma V^{\mathbf{n}} = V_2^{\mathbf{n}} + V_3^{\mathbf{n}}$$

Thus the system of equations can be rewritten as

$$\left(\begin{array}{cc|c} h_{11} & h_{12} & 0 \\ h_{21} & h_{22} & 0 \\ \hline h_{31} & h_{32} & 0 \end{array}\right)\left(\begin{array}{c} \Omega_1 \\ \Delta V \\ \hline 0 \end{array}\right) = \left(\begin{array}{cc|c} g_{11} & g_{12} & 0 \\ g_{21} & g_{22} & 0 \\ \hline g_{31} & g_{32} & 0 \end{array}\right)\left(\begin{array}{c} \hat{\Omega}_1 \\ \Sigma V^{\mathbf{n}} \\ \hline 0 \end{array}\right) \tag{14}$$

It therefore suffices to solve the smaller 2×2 block system for the unknowns $(\Omega_1, \Delta V)$.

In the simple BEM approach, as explained earlier, the boundary conditions of the original problem have to be incorporated in the modified boundary value problem. As shown in Section 2.3, the Neumann boundary condition of the original problem changes to a Robin boundary condition. Typically the crack surfaces are subjected to Neumann boundary conditions. If the known flux on the two crack surfaces is denoted by $\overline{q_2}$ and $\overline{q_3}$ then, according to Equation (9), $\Sigma V^{\mathbf{n}}$ in Equation (14) changes to

$$\Sigma V^{\mathbf{n}} = \frac{1}{2k}\frac{\partial k}{\partial \mathbf{n}}(V_2 + V_3) - \frac{\overline{q_2} + \overline{q_3}}{\sqrt{k}} \tag{15}$$

Copyright © 2005 John Wiley & Sons, Ltd.

Therefore, Equation (14) is rewritten as

$$\left(\begin{array}{cc|c} h_{11} & h_{12} & 0 \\ h_{21} & h_{22} & 0 \\ \hline h_{31} & h_{32} & 0 \end{array}\right)\left(\begin{array}{c} \Omega_1 \\ \hline V_2 - V_3 \\ 0 \end{array}\right) = \left(\begin{array}{cc|c} g_{11} & g_{12} & 0 \\ g_{21} & g_{22} & 0 \\ \hline g_{31} & g_{32} & 0 \end{array}\right)\left(\begin{array}{c} \hat{\Omega}_1 \\ \hline \dfrac{1}{2k}\dfrac{\partial k}{\partial \mathbf{n}}(V_2 + V_3) - \dfrac{\overline{q_2} + \overline{q_3}}{\sqrt{k}} \\ 0 \end{array}\right) \tag{16}$$

Due to this change in the system of equations it is apparent from Equation (16) that the unknown variable can no longer be the jump in potential $\Delta V = V_2 - V_3$. As a result, the standard displacement discontinuity approach is not directly suitable as a fracture algorithm for the simple BEM technique.

3.2. The dual BEM approach

The dual BEM approach is the method of choice to solve fracture problems in this work. In this technique, Equation (13) is used after modifying the boundary conditions. This is suitable for problems in potential theory because for these problems the variable of interest is the potential distribution on the crack surfaces. In the dual BEM approach, the potentials are calculated directly during the solution process. On the contrary, in the displacement discontinuity approach, the variable that is obtained from the system of equations is the jump in potential. As a consequence, postprocessing and assembling the h_{31} and h_{32} are required. The system of equations (before incorporating the treatment of boundary conditions) is

$$\begin{pmatrix} h_{11} & h_{12} & -h_{12} \\ h_{21} & h_{22} & -h_{22} \\ h_{31} & h_{32} & -h_{32} \end{pmatrix}\begin{pmatrix} \Omega_1 \\ V_2 \\ V_3 \end{pmatrix} = \begin{pmatrix} g_{11} & g_{12} & g_{12} \\ g_{21} & g_{22} & g_{22} \\ g_{31} & g_{32} & g_{32} \end{pmatrix}\begin{pmatrix} \hat{\Omega}_1 \\ V_2^{\mathbf{n}} \\ V_3^{\mathbf{n}} \end{pmatrix} \tag{17}$$

Note the relationship between the columns 2 and 3 of the matrix. As a result, only the upper (or lower) crack surface needs to be discretized and corresponding kernels need to be calculated. Finally, during the solution phase, the system of equations is assembled by including the kernels corresponding to the other crack surface.

Remark

Note that, for the non-crack boundary the BIE can be employed instead of the HBIE. The reason behind choosing the HBIE over the BIE is that the present code is written in such a way that while solving homogeneous problems the code works as a symmetric Galerkin BEM [11] for which the HBIE is applied to the surface with Neumann boundary conditions.

4. NUMERICAL IMPLEMENTATION

Numerical implementation for specific cases using the variations of $k(x, y, z)$ in one co-ordinate are presented. In the present paper only parabolic k-variation has been considered although exponential and trigonometric material variation can be dealt with in similar fashion [26]. The numerical methods employed in the current work use Galerkin techniques for the BIE and HBIEs. A brief discussion of these techniques in the context of the BEM is presented below. It

Copyright © 2005 John Wiley & Sons, Ltd.

also includes the development of the Galerkin boundary conditions, selection of the boundary element type, treatment of singular integrals and corners.

4.1. Galerkin boundary integral equation

Define the collocation BIE as

$$\mathscr{B}(P) \equiv v(P) + \int_\Gamma \left(\frac{\partial}{\partial \mathbf{n}} G(P, Q) \right) v(Q)\, \mathrm{d}Q - \int_\Gamma G(P, Q) \frac{\partial v}{\partial \mathbf{n}} (Q)\, \mathrm{d}Q \tag{18}$$

and thus for an exact solution $\mathscr{B}(P) \equiv 0$. Here $\mathbf{n} = \mathbf{n}(Q)$, $\mathbf{N} = \mathbf{N}(P)$ denote the unit outward normal on the boundary surface Γ, and P and Q are points on Γ (see Figure 1).

In a Galerkin approximation, shape functions (ψ_k) are employed as weighting functions for enforcing the integral equations [48], and Equation (18) takes the form (see Figure 3)

$$\int_\Gamma \psi_k(P) \mathscr{B}(P)\, \mathrm{d}P = 0 \tag{19}$$

4.2. Galerkin hypersingular boundary integral equation

The hypersingular boundary integral equation for the Laplace equation $\nabla^2 v = 0$ is an expression for the surface flux $\partial v / \partial \mathbf{n} = \nabla v \bullet \mathbf{n}$, usually written in the form

$$\frac{\partial v}{\partial \mathbf{N}}(P) + \int_\Gamma v(Q) \frac{\partial^2 G}{\partial \mathbf{N} \partial \mathbf{n}} (P, Q)\, \mathrm{d}Q - \int_\Gamma \frac{\partial G}{\partial \mathbf{N}} (P, Q) \frac{\partial v}{\partial \mathbf{n}} (Q)\, \mathrm{d}Q = 0 \tag{20}$$

The fundamental solution $G(P, Q)$ is usually taken as the point source potential (for homogeneous media):

$$G(P, Q) = \frac{1}{4\pi r} \tag{21}$$

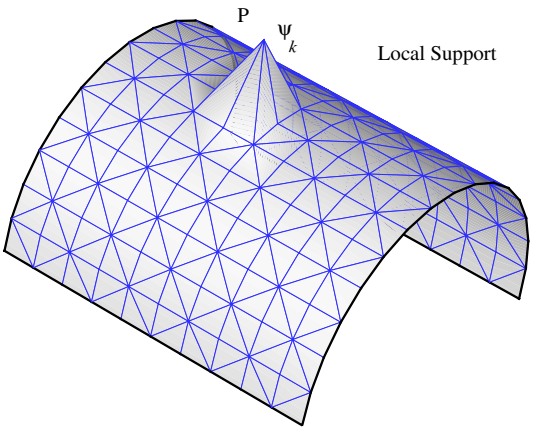

Figure 3. Local support for the Galerkin BEM.

Copyright © 2005 John Wiley & Sons, Ltd.

where $\mathbf{R} = \mathbf{Q} - \mathbf{P}$ and $r = \|\mathbf{R}\|$ is the distance between points P and Q. The expressions of the derivatives of the Green's function with respect to the normals $\mathbf{n}$ and $\mathbf{N}$ are

$$\frac{\partial G}{\partial \mathbf{n}}(P, Q) = -\frac{1}{4\pi}\frac{\mathbf{n}\bullet\mathbf{R}}{r^3} \tag{22}$$

and

$$\frac{\partial G}{\partial \mathbf{N}}(P, Q) = \frac{1}{4\pi}\frac{\mathbf{N}\bullet\mathbf{R}}{r^3} \tag{23}$$

The hypersingular kernel is therefore given by

$$\frac{\partial^2 G}{\partial \mathbf{N}\partial \mathbf{n}}(P, Q) = \frac{1}{4\pi}\left(\frac{\mathbf{n}\bullet\mathbf{N}}{r^3} - 3\frac{(\mathbf{n}\bullet\mathbf{R})(\mathbf{N}\bullet\mathbf{R})}{r^5}\right) \tag{24}$$

It is important to note that Equation (20) is formally obtained by differentiating the standard BIE for surface potential, and then interchanging the derivative with the integral. As there are no singularities, the interchange is permitted, and the limit as P returns to the boundary can then be considered. This limit process will be employed below. A side benefit of the direct limit procedure is that, if the limit is taken with the source point P approaching the boundary from *outside* the domain, then the 'free term' $\partial v(P)/\partial \mathbf{N}$ from Equation (20) is not present. Thus if we define the hypersingular BIE (flux BIE) as

$$\mathscr{F}(P) \equiv \int_\Gamma v(Q)\frac{\partial^2 G}{\partial \mathbf{N}\partial \mathbf{n}}(P, Q)\,\mathrm{d}Q - \int_\Gamma \frac{\partial G}{\partial \mathbf{N}}(P, Q)\frac{\partial v}{\partial \mathbf{n}}(Q)\,\mathrm{d}Q \tag{25}$$

then Equation (20) takes the form

$$\mathscr{F}(P) = 0 \tag{26}$$

with the free term automatically incorporated in the *exterior limit* evaluation of the second integral in Equation (25).

Following the Galerkin approximation, the flux BIE, Equation (26), takes the form

$$\int_\Gamma \psi_k(P)\mathscr{F}(P)\,\mathrm{d}P = 0 \tag{27}$$

where ψ_k are the usual Galerkin weighting functions (see Equation (19)). As a result the Galerkin technique possesses the important property of the *local support* (see Figure 3).

4.3. Interpolation of physical variables

Following standard practice, the boundary potential and flux are approximated in terms of values at element nodes Q_j and shape functions $\psi_j(Q)$, i.e.

$$v(Q) = \sum_j \psi_j(Q)v(Q_j) \tag{28}$$

$$\frac{\partial v}{\partial \mathbf{n}}(Q) = \sum_j \psi_j(Q)\frac{\partial v}{\partial \mathbf{n}}(Q_j) \tag{29}$$

Notice that the same shape functions are used to define both potential and flux.

Copyright © 2005 John Wiley & Sons, Ltd.

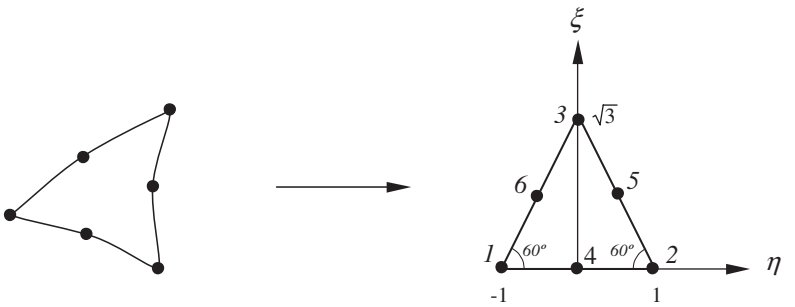

Figure 4. A triangle in the 3D space is mapped to an equilateral triangular quadratic element in $\{\eta, \xi\}$ space.

4.4. Boundary elements

The surface of the solution domain is divided into a number of connected elements. Over each element, the variation of the geometry and the variables (potential and flux) is approximated by polynomial functions. Six noded isoparametric quadratic triangular elements are used in the present work (see Figure 4).

The geometry of an element can be defined by the co-ordinates of its six nodes using appropriate quadratic shape functions as follows:

$$x_i(\eta, \xi) = \sum_{j=1}^{6} N_j(\eta, \xi)(x_i)_j \tag{30}$$

By means of an isoparametric approximation, the same shape functions are used for the solution variables (both potential and flux), as follows:

$$v_i(\eta, \xi) = \sum_{j=1}^{6} N_j(\eta, \xi)(v_i)_j \tag{31}$$

$$\frac{\partial v_i}{\partial \mathbf{n}}(\eta, \xi) = \sum_{j=1}^{6} N_j(\eta, \xi)\left(\frac{\partial v_i}{\partial \mathbf{n}}\right)_j \tag{32}$$

The shape functions can be explicitly written in terms of intrinsic co-ordinates η and ξ as (see Figure 4):

$$\begin{aligned} &N_1(\eta, \xi) = (\xi + \sqrt{3}\eta - \sqrt{3})(\xi + \sqrt{3}\eta)/6, \quad N_4(\eta, \xi) = (\xi + \sqrt{3}\eta - \sqrt{3})(\xi - \sqrt{3}\eta - \sqrt{3})/3 \\ &N_2(\eta, \xi) = (\xi - \sqrt{3}\eta - \sqrt{3})(\xi - \sqrt{3}\eta)/6, \quad N_5(\eta, \xi) = -2\xi(\xi - \sqrt{3}\eta - \sqrt{3})/3 \\ &N_3(\eta, \xi) = \xi(2\xi - \sqrt{3})/3, \quad N_6(\eta, \xi) = -2\xi(\xi + \sqrt{3}\eta - \sqrt{3})/3 \end{aligned} \tag{33}$$

The intrinsic co-ordinate space is the equilateral triangle with $-1 \leqslant \eta \leqslant 1$, $0 \leqslant \xi \leqslant \sqrt{3}(1 - |\eta|)$. The range of co-ordinates has been chosen for the sake of ease of computational implementation when dealing with singular integration [38].

Copyright © 2005 John Wiley & Sons, Ltd.

4.5. Treatment of boundary conditions

With respect to standard BEM codes the main modification in the implementation of the simple BEM consists of incorporating the boundary conditions for the modified problem. In this section, the necessary modifications are described.

For the sake of illustration, let us assume three nodes, of which nodes 1 and 3 have prescribed Neumann boundary condition, and node 2 has prescribed Dirichlet boundary condition, i.e.

$$\begin{aligned} &\overline{q_1},\ \overline{\phi_2},\ \overline{q_3} \quad \text{known quantities} \\ &\phi_1,\ q_2,\ \phi_3 \quad \text{unknown quantities} \end{aligned}$$

In the modified boundary value problem the variables are v and $\partial v/\partial \mathbf{n}$ (see Equations (8) and (9), respectively). The system of algebraic equations emerges as

$$\begin{bmatrix} H_{11} & H_{12} & H_{13} \\ H_{21} & H_{22} & H_{23} \\ H_{31} & H_{32} & H_{33} \end{bmatrix} \begin{Bmatrix} v_1 \\ v_2 \\ v_3 \end{Bmatrix} = \begin{bmatrix} G_{11} & G_{12} & G_{13} \\ G_{21} & G_{22} & G_{23} \\ G_{31} & G_{32} & G_{33} \end{bmatrix} \begin{Bmatrix} \partial v_1/\partial \mathbf{n} \\ \partial v_2/\partial \mathbf{n} \\ \partial v_3/\partial \mathbf{n} \end{Bmatrix} \tag{34}$$

By rearranging the equations so that the unknowns are passed to the left-hand side, we rewrite the linear system as follows:

$$\begin{bmatrix} H_{11} & -G_{12} & H_{13} \\ H_{21} & -G_{22} & H_{23} \\ H_{31} & -G_{32} & H_{33} \end{bmatrix} \begin{Bmatrix} v_1 \\ \partial v_2/\partial \mathbf{n} \\ v_3 \end{Bmatrix} = \begin{bmatrix} G_{11} & -H_{12} & G_{13} \\ G_{21} & -H_{22} & G_{23} \\ G_{31} & -H_{32} & G_{33} \end{bmatrix} \begin{Bmatrix} \partial v_1/\partial \mathbf{n} \\ v_2 \\ \partial v_3/\partial \mathbf{n} \end{Bmatrix} \tag{35}$$

Using Equations (8) and (9), we obtain the final form of the system of equations,

$$\begin{bmatrix} \left(H_{11} - \dfrac{G_{11}}{2k}\dfrac{\partial k}{\partial \mathbf{n}}\right) & -G_{12} & \left(H_{13} - \dfrac{G_{13}}{2k}\dfrac{\partial k}{\partial \mathbf{n}}\right) \\ \left(H_{21} - \dfrac{G_{21}}{2k}\dfrac{\partial k}{\partial \mathbf{n}}\right) & -G_{22} & \left(H_{23} - \dfrac{G_{23}}{2k}\dfrac{\partial k}{\partial \mathbf{n}}\right) \\ \left(H_{31} - \dfrac{G_{31}}{2k}\dfrac{\partial k}{\partial \mathbf{n}}\right) & -G_{32} & \left(H_{33} - \dfrac{G_{33}}{2k}\dfrac{\partial k}{\partial \mathbf{n}}\right) \end{bmatrix} \begin{Bmatrix} v_1 \\ \partial v_2/\partial \mathbf{n} \\ v_3 \end{Bmatrix}$$

$$= \begin{bmatrix} G_{11} & -H_{12} & G_{13} \\ G_{21} & -H_{22} & G_{23} \\ G_{31} & -H_{32} & G_{33} \end{bmatrix} \begin{Bmatrix} -\overline{q_1}/\sqrt{k} \\ \overline{\phi_2}\sqrt{k} \\ -\overline{q_3}/\sqrt{k} \end{Bmatrix} \tag{36}$$

Copyright © 2005 John Wiley & Sons, Ltd.

We solve these equations for v_1, $\partial v_2/\partial \mathbf{n}$, and v_3; and finally, by using Equations (8) and (9), we obtain

$$\begin{aligned} \phi_1 &= v_1/\sqrt{k} \\ q_2 &= -\sqrt{k}\left\{\frac{\partial v_2}{\partial \mathbf{n}} - \frac{1}{2k}\frac{\partial k}{\partial \mathbf{n}} v_2\right\} \\ \phi_3 &= v_3/\sqrt{k} \end{aligned} \tag{37}$$

4.6. Singular integrals

In a Galerkin approximation, the integration is carried out with respect to both the field point Q and the source point P (see Figure 1). In the numerical implementation, the integrals are evaluated for every pair of elements. Singular integrals take place as the Green's function and its derivatives diverge when the field point approaches the source point. An integral is therefore singular if the elements are *coincident*, or are *adjacent*, sharing either an edge or a vertex. Thus, for three-dimensional problems, there are four typical configurations for the two elements containing the source point P and the field point Q (see Figure 5), and thus four distinct situations regarding the singularity must be considered:

- Non-singular case. When the source point P and the field point Q lie on distinct elements, that do not share a common vertex or edge.
- Coincident case. When the source point P and the field point Q lie in the same element.
- Edge adjacent case. When two elements share a common edge.
- Vertex adjacent case. When a vertex is the only common node between the two elements.

A hybrid analytical/numerical approach using the 'limit to the boundary' approach is adopted to treat the singular integrals. The non-singular integrals can be evaluated using standard

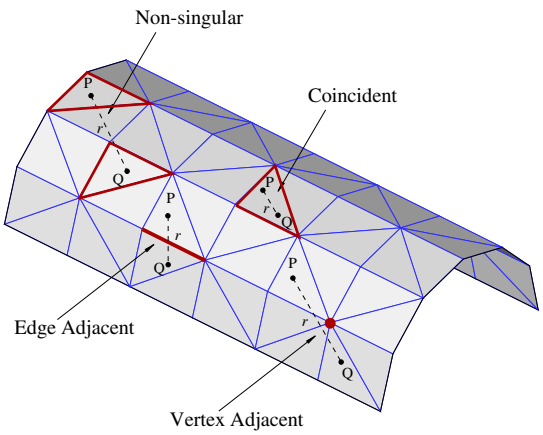

Figure 5. Four different cases considered for integration: (a) non-singular; (b) coincident; (c) edge adjacent; and (d) vertex adjacent.

Copyright © 2005 John Wiley & Sons, Ltd.

Gaussian quadrature formulas. In the 'limit to the boundary' approach for evaluating the singular integrals, the integrals for the coincident and the edge-adjacent cases are forced to be finite by moving the source P off the boundary in the direction $\mathbf{N}$ at a distance ε. The next step is to employ polar co-ordinate transformations and then integrate analytically with a *fixed distance from the singularity*. After the exact integration, the limit $\varepsilon \to 0$ is considered. The coincident and the edge-adjacent hypersingular integrals are separately divergent, producing terms of the form $\log(\varepsilon)$. However, the divergent terms from the coincident case cancels out with the divergent terms from the edge-adjacent case, and therefore the divergent terms are removed exactly in this approach. Taking the limit $\varepsilon \to 0$ back to the boundary results in finite expressions, thus giving a well behaved integral. Once the divergent terms have been identified and removed, the remaining terms of the integral can be evaluated using standard numerical quadrature. In the vertex adjacent case, the singularity is limited to a single point in the four dimensional integration (see Figure 5(d)). The integral does not produce a divergent term. A number of transformations and analytical integration(s) are carried out to treat this integral. Details of this technique can be found in the papers by Sutradhar *et al.* [38] and Gray *et al.* [49].

4.7. Corners

The treatment of corners in the GBEM is simple and elegant due to the flexibility in choosing the weight function for the Galerkin approximation [14]. Corners are represented by multiple nodes [50], and on each side different weight functions are used (see Figure 6) [14]. Figure 6 shows an assembly of six planes with different orientation of the normals where, each plane

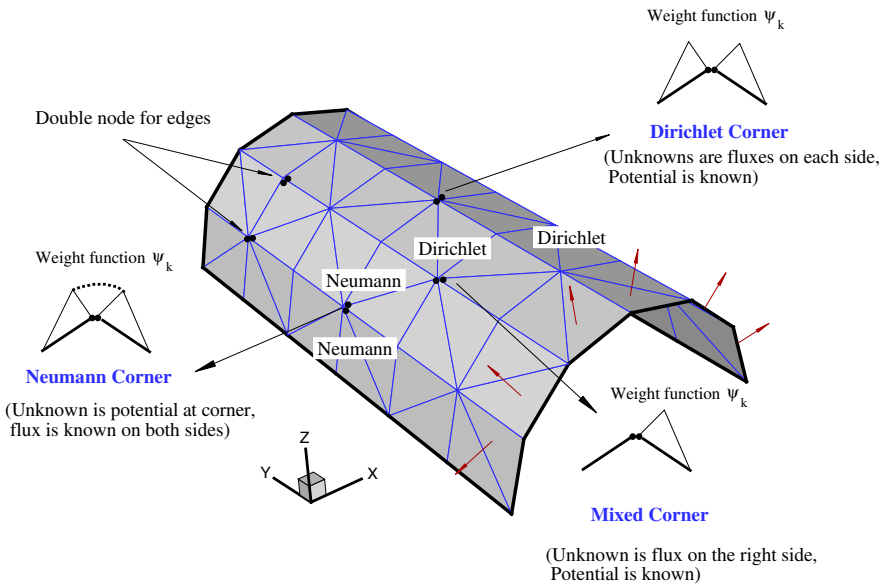

Figure 6. Corner treatment in the Galerkin BEM. Notice that the six normal vectors in the figure define the six planes that compose the semi-cylindrical geometry (with axis along the y direction).

Copyright © 2005 John Wiley & Sons, Ltd.

has been prescribed with either Dirichlet or Neumann boundary conditions. Consequently at the intersection of two planes double nodes are applied. For a mixed corner (flux is unknown in one side of the corner, potential is known), a non zero weight function is assigned only on the side where flux is unknown. For a Neumann corner (flux specified on both sides of the corner, potential is the unknown), the weight functions are combined together. On a Dirichlet corner (unknowns are flux on each sides, potential is known) the usual weight functions are assigned on both sides of the corners. The formulation is capable of treating situations when multiple planes meet at the corners [26, 27].

5. NUMERICAL EXAMPLES

In this section, a number of numerical problems are reported to demonstrate the implementation of the techniques described above. To verify the numerical implementation, the following three examples are presented

(1) A penny-shaped crack inside a cylinder.
(2) Three parallel penny-shaped crack inside a cylinder.
(3) Multiple random cracks inside a cube.

The first problem is a penny-shaped crack inside a cylinder with constant temperature on two sides and insulated on the wall. The material property varies quadratically only in the z direction. The second problem has three parallel penny-shaped cracks inside a cylinder with same outer boundary conditions and gradation as the first problem. The last example is a complicated 3D problem with multiple random cracks inside a cube. This example demonstrates the efficiency and robustness of the BEM formulation and the code. The conductivity varies gradually along the z direction. Other material property variations can be considered by using the present methodology to handle cracks in the simple BEM (see Sections 2–4) and Reference [26].

5.1. Penny-shaped crack inside a cylinder

A cylinder with dimensions of (radius $= 1.476$, height $= 3$) is considered as shown in Figure 7. The radius of the penny-shaped crack is 0.5 unit. The top surface of the cylinder at $[z = 1]$ is maintained at a temperature of $T = 100$ while the bottom is maintained at $T = 0$. The cylindrical wall is insulated. The crack surfaces are insulated. The quadratic variation of the thermal conductivity $k(x, y, z)$ is defined as (see Table I)

$$k(x, y, z) = k(z) = k_0(a_1 + \beta z)^2 = 5(1 + \beta z)^2 \tag{38}$$

in which β is the non-homogeneity parameter. Notice that β has units of $1/[\text{length}]$, and this $1/\beta$ represents the length scale of material non-homogeneity. The BEM results are compared with results from finite element simulations. The BEM mesh consisting of 1736 elements and 3664 nodes is shown in Figure 8. The FEM mesh consisting of 6680 brick and tetrahedral crack-tip elements, and 27 310 nodes is shown is Figure 9. In the present work, in order to incorporate the functional variation of the material at the finite element level, the user subroutine UMATHT developed for the FEM software ABAQUS [51] is used [25]. By means of this subroutine, any functional variation can be included within an element by sampling the material property at each Gauss point. The temperature distribution along the radial distance

Copyright © 2005 John Wiley & Sons, Ltd.

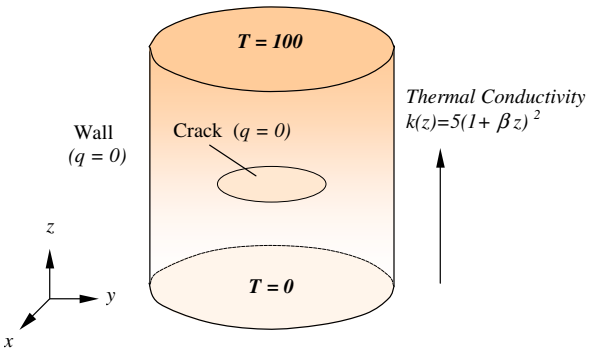

Figure 7. Geometry and boundary condition for penny-shaped crack inside a cylinder.

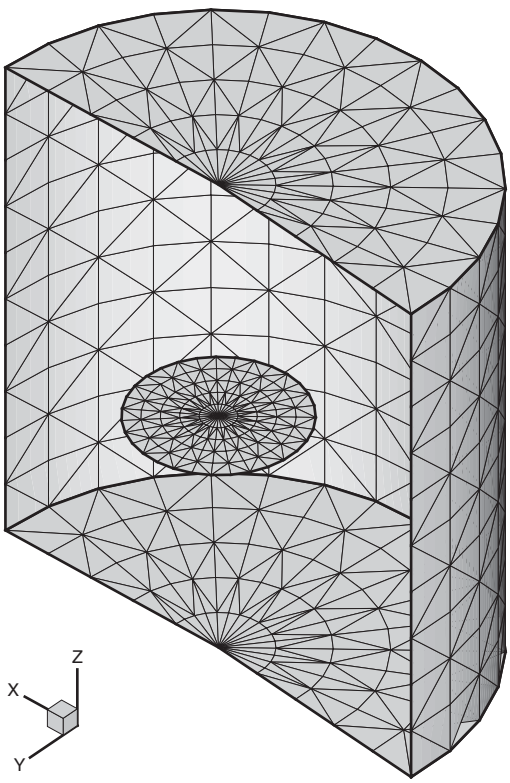

Figure 8. Illustration of the BEM mesh for penny-shaped crack inside a cylinder (1736 elements and 3664 nodes). The cylinder is clipped for visualization purpose.

from the centre of the crack for both the upper and the lower crack surfaces for different values of β, for the BEM simulations are shown in Figures 10–12. The BEM and FEM results match very well. A contour plot of the temperature for the upper crack surface comparing the

Copyright © 2005 John Wiley & Sons, Ltd.

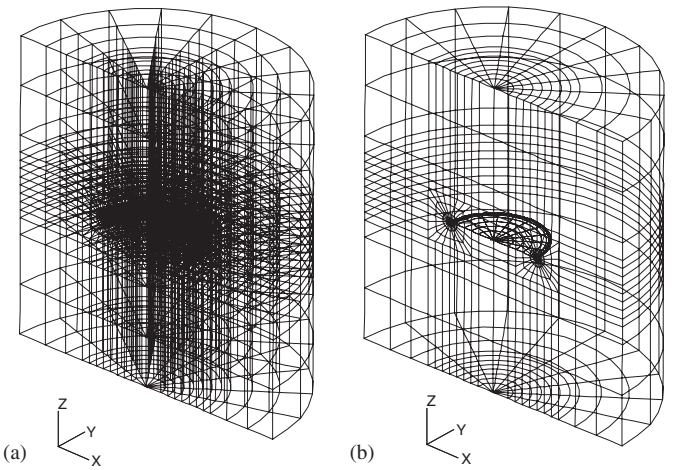

Figure 9. Illustration of FEM mesh for penny-shaped crack inside a cylinder (6680 elements and 27 310 nodes): (a) half mesh; and (b) surface-only display.

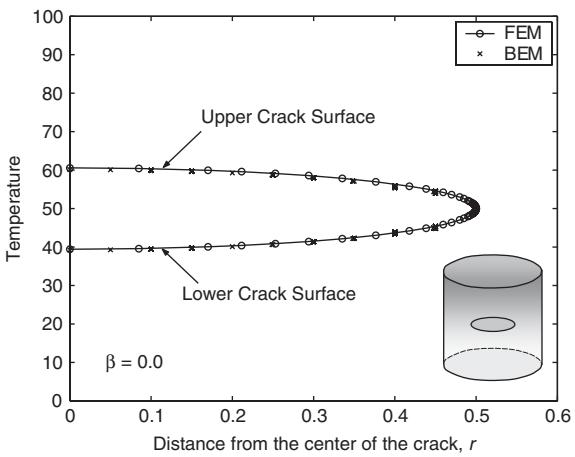

Figure 10. Temperature along radial distance from the centre of the crack for $\beta = 0.0$ (homogeneous media).

BEM and the FEM results in Figure 13. Finally, Figure 14 depicts a contour plot showing the temperature distribution on the clipped cylindrical wall.

5.2. Three parallel penny-shaped cracks inside a cylinder

The cylinder of the previous example is considered again, but now there are three parallel cracks (radius of each crack $= 0.5$ unit) as shown in Figure 15. The outer boundary conditions and the material gradation are the same as in the previous example. The crack surfaces

Copyright © 2005 John Wiley & Sons, Ltd.

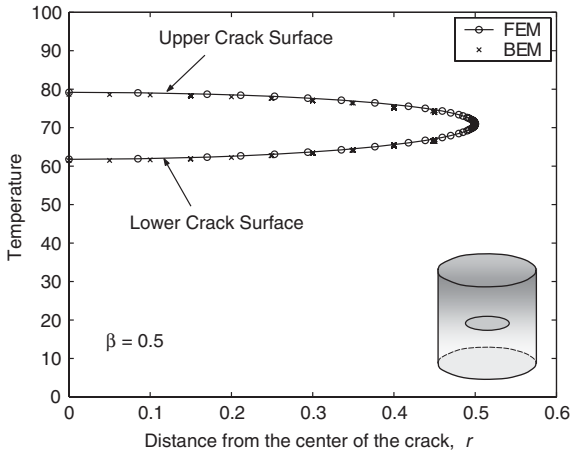

Figure 11. Temperature along radial distance from the centre of the crack for $\beta = 0.5$ (graded medium).

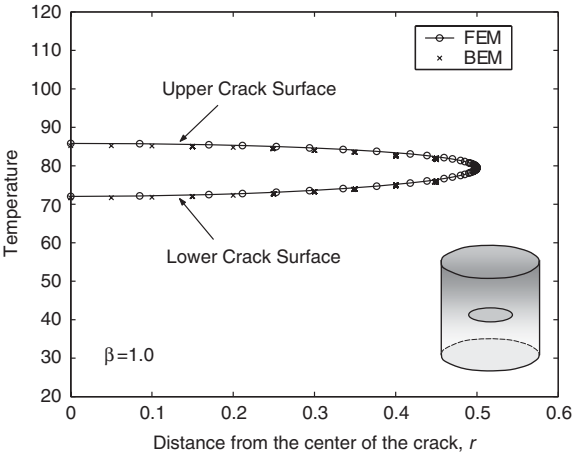

Figure 12. Temperature along radial distance from the centre of the crack for $\beta = 1.0$ (graded medium).

are insulated. The BEM mesh consisting of 2852 elements and 6024 nodes is illustrated in Figure 16. Again, for this example, the BEM results are compared with results from finite element simulations. The FEM mesh consisting of 16 080 brick and tetrahedral crack-tip elements and 64 732 nodes is shown is Figure 17(a). Figure 17(b) shows the overall FEM mesh which depicts the complexity of the meshing effort. A section through the crack front is taken in Figure 17(c) in order to show the finer mesh distribution along the crack front. The temperature distribution along the radial distance from the centre of the crack for both the upper and the lower crack surfaces, for different values of β, are shown in Figures 18–20. The BEM and

Copyright © 2005 John Wiley & Sons, Ltd.

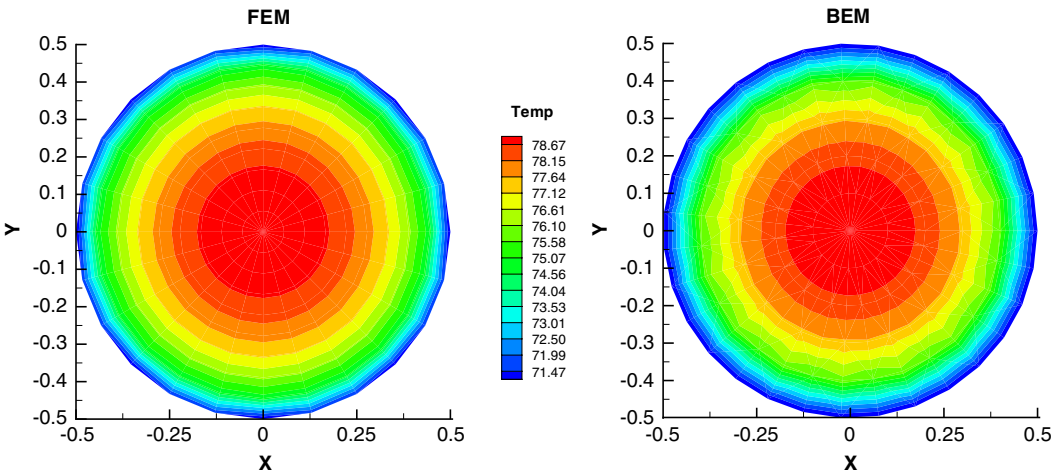

Figure 13. Comparison of contour plots of temperature for the FEM and BEM results for the lower crack surface for $\beta = 1.0$.

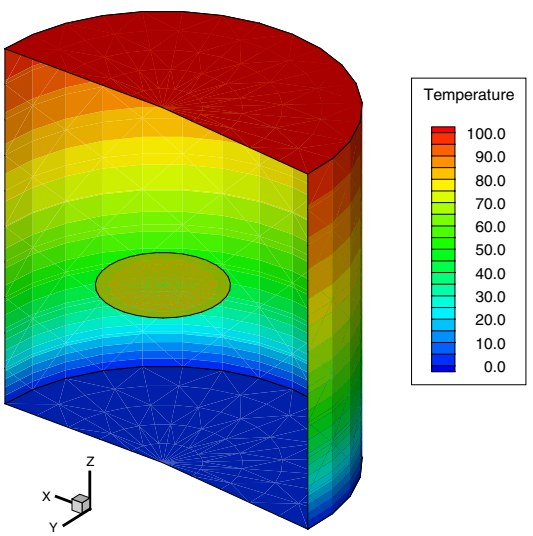

Figure 14. A contour plot showing the temperature distribution obtained from BEM on the wall and on the crack surface for $\beta = 0.5$.

FEM results match very well for this multiple crack problem in a finite geometry. Contour plots of the temperature distribution on both the upper and the lower crack surfaces for the top, middle and the bottom cracks considering $\beta = 1.0$, are shown in Figure 21, which illustrates the spatial distribution of temperature.

Copyright © 2005 John Wiley & Sons, Ltd.

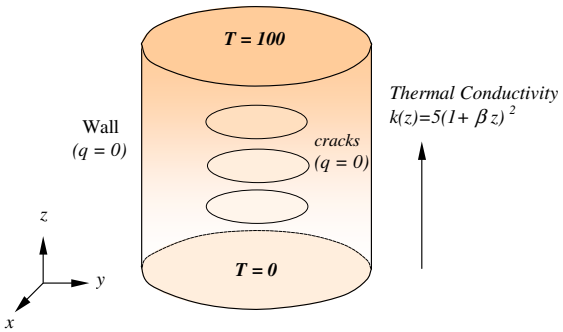

Figure 15. Geometry and boundary condition of three penny-shaped cracks inside a cylinder.

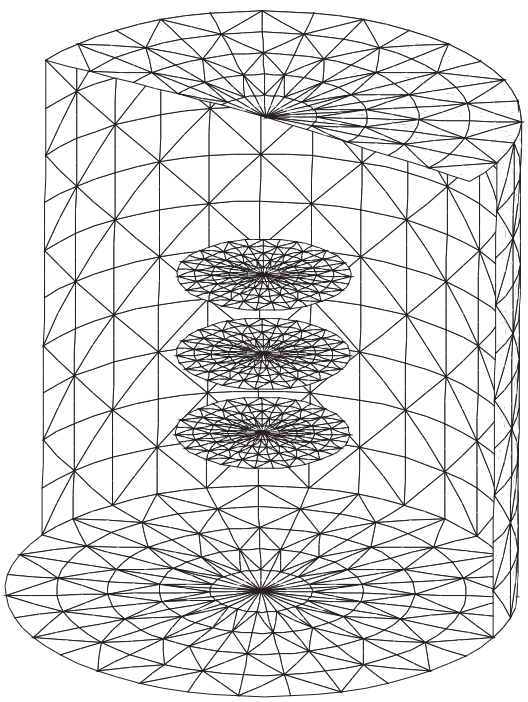

Figure 16. BEM mesh for three penny-shaped crack inside a cylinder with 2852 elements and 6024 nodes. The cylinder is clipped for visualization purpose.

5.3. Multiple random cracks inside a cube

In this example, eleven cracks of circular and elliptical shapes are randomly oriented inside a cube. The thermal conductivity variation is

$$k(x, y, z) = 5(1 + 1.5z)^2 \tag{39}$$

Copyright © 2005 John Wiley & Sons, Ltd.

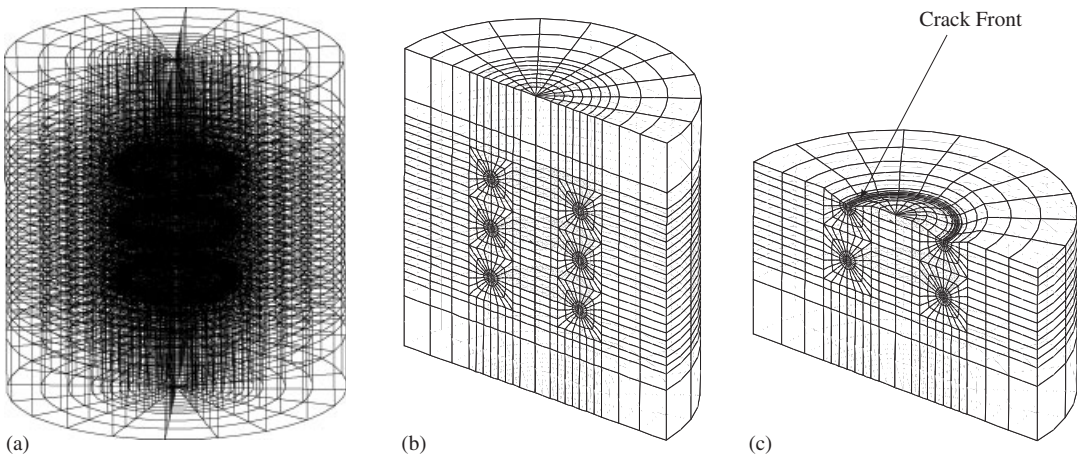

Figure 17. The FEM mesh for three penny-shaped cracks inside a cylinder (16 080 elements and 28 732 nodes): (a) mesh discretization; (b) section through the middle of the FEM mesh only showing the surface of the elements; and (c) section through the crack plane showing the mesh around the crack front.

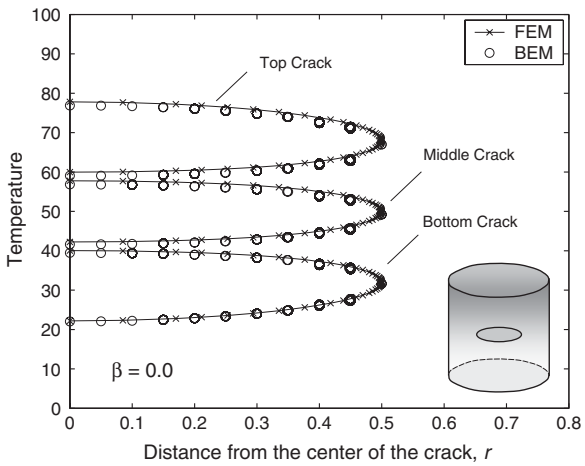

Figure 18. Temperature distribution along radial distance from the centre for $\beta = 0.0$ on the three cracks inside a cylinder.

The boundary conditions prescribed for this problem is similar to the previous examples i.e. the top surface of the cube at $[z = 1]$ is maintained at a temperature of $T = 100$ while the bottom is maintained at $T = 0$, and the remaining four walls are insulated. The crack surfaces are insulated. The outer cube geometry and the BEM mesh on the cracks are shown in Figure 22. The BEM mesh consists of only 900 elements and 2033 nodes. Contour plots showing usage of clippers for visualizing the upper temperature of the crack surfaces are shown in Figure 23(a)–(c). The flux distribution for the upper $[z = 1]$ and the lower $[z = 0]$

Copyright © 2005 John Wiley & Sons, Ltd.

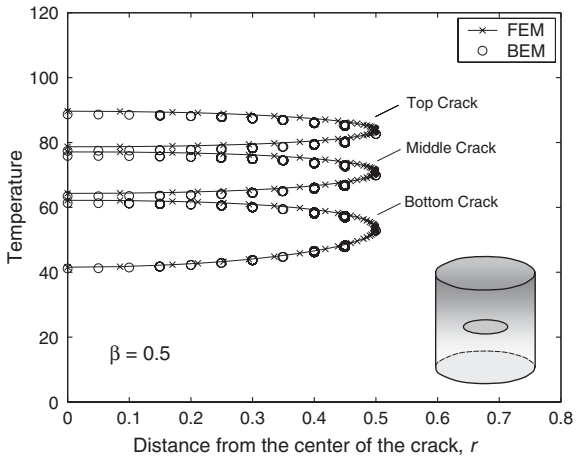

Figure 19. Temperature distribution along radial distance from the centre for $\beta = 0.5$ on the three cracks inside a cylinder.

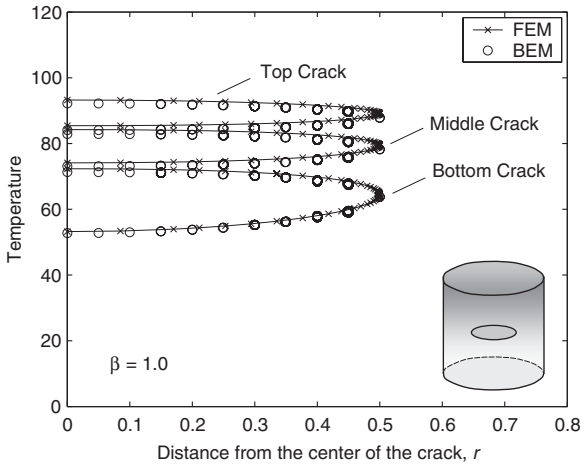

Figure 20. Temperature distribution along radial distance from the centre for $\beta = 1.0$ on the three cracks inside a cylinder.

plane of the cube is shown in Figure 24, which shows the presence of the multiple cracks influences the resulting flux on these planes. A complicated problem such as this would be very tedious to mesh using three-dimensional finite elements. This problem demonstrates the robustness of the present simulation. The code can handle any number of cracks of different sizes and shapes.

Copyright © 2005 John Wiley & Sons, Ltd.

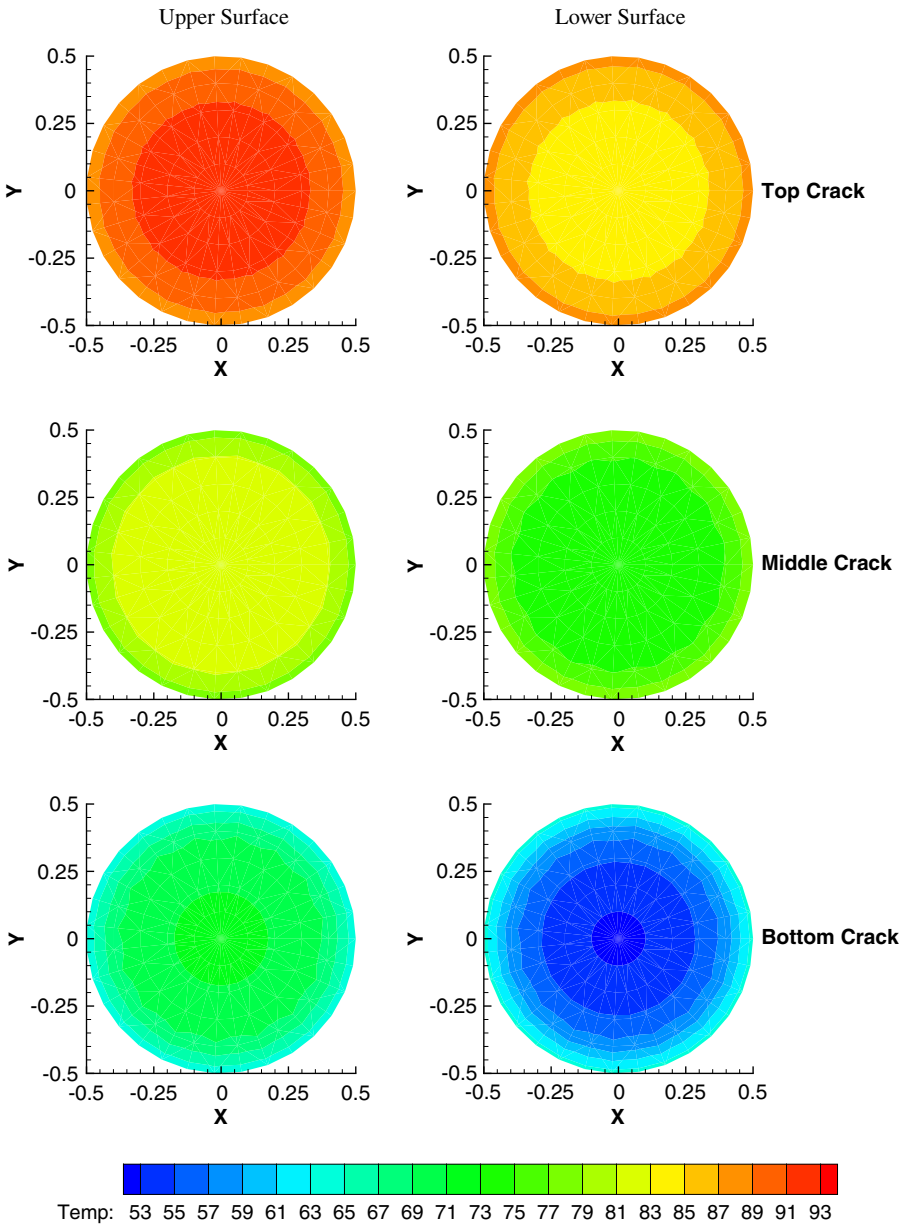

Figure 21. BEM temperature distribution on the upper (left) and lower (right) crack surfaces for the top, middle and bottom crack. The material non-homogeneity parameter $\beta = 1.0$.

Copyright © 2005 John Wiley & Sons, Ltd.

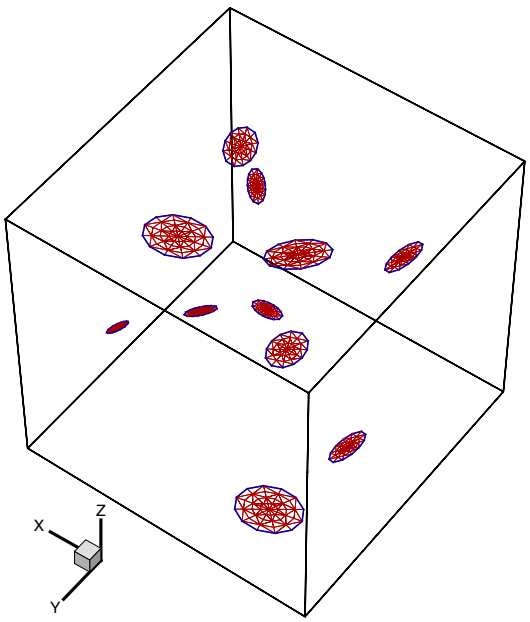

Figure 22. Multiple cracks inside a cube. The complete BEM mesh consists of 900 elements and 2033 nodes.

6. CONCLUSIONS AND EXTENSIONS

In the 'simple BEM', problems in non-homogeneous media are transformed to known problems in homogeneous media such that existing codes (for homogeneous media) can be reused with straightforward modifications. A 'simple BEM' for solving multiple cracks in problems governed by potential theory is presented herein. Steady-state heat conduction problems with functionally graded thermal conductivity are investigated. Numerical problems with single and multiple interacting cracks are solved, and the BEM results are verified by means of the FEM. A numerical example consisting of several random cracks of various sizes and shapes is presented to demonstrate the robustness of the present BEM formulation and implementation. A quadratic variation of thermal conductivity was considered in the examples, however, other gradations, such as trigonometric and exponential, can be readily solved by employing the technique. In the formulation, if the jump in potential is used as the primary variable on the crack surface, then the displacement discontinuity approach is not directly applicable. The dual BEM, which employs the potential as the primary variable on the crack surfaces, is more suitable to treat the fracture problem for non-homogeneous media using the 'simple BEM'.

The present 'simple BEM' leads naturally to several extensions. Although only interior problems were addressed, exterior problems can be treated on a similar fashion [52]. In addition, fracture problems involving transient heat conduction with constant diffusivity can be easily solved by employing the Laplace transform technique of Sutradhar and Paulino [27]. The present formulation also offers room for extension to graded orthotropic media [53, 54]. These and other related problems are presently under consideration by the authors.

Copyright © 2005 John Wiley & Sons, Ltd.

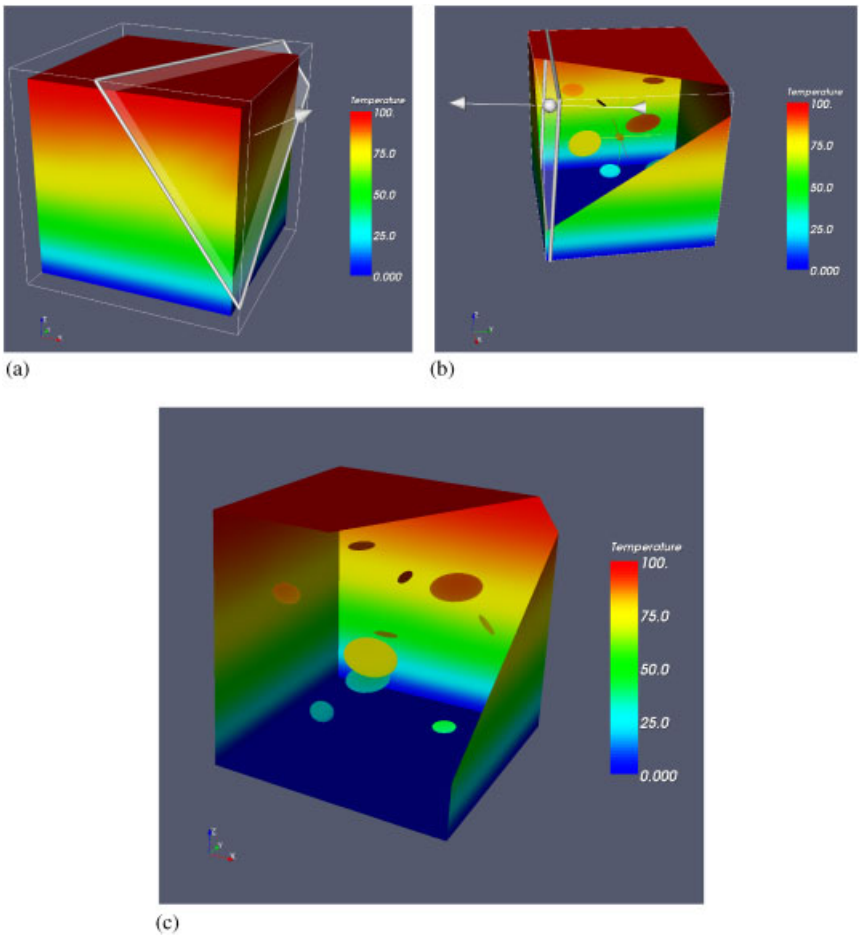

Figure 23. (a) Temperature distribution on the wall with a clip plane applied; (b) clipped cube; and (c) clipped cube showing the temperature distribution of the upper crack surfaces and walls.

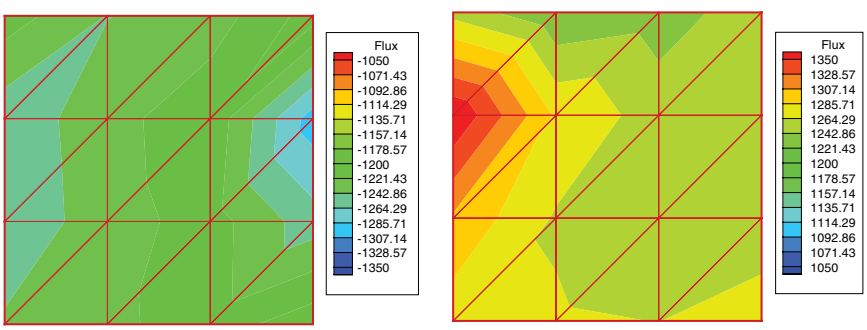

Figure 24. BEM flux distribution on the $z = 1$ (left) and $z = 0$ (right) plane of the cube.

Copyright © 2005 John Wiley & Sons, Ltd.

ACKNOWLEDGEMENTS

We acknowledge the support from the Computational Science and Engineering (CSE) Program (Prof. Michael Heath, Director) at the University of Illinois at Urbana-Champaign (UIUC) for the CSE Fellowship award to A. Sutradhar. G. H. Paulino acknowledges the support from the National Science Foundation under grant CMS-0115954 (Mechanics and Materials Program). We also would like to thank Dr. Matthew C. Walters (UIUC) for help with the finite element meshes.

REFERENCES

1. Medina DE, Liggett JA. Three dimensional boundary element computation of potential flow in fractured rock. *International Journal for Numerical Methods in Engineering* 1988; **26**:2319–2330.
2. Shapiro AM, Andersson J. Steady state fluid response in fractured rock: a boundary element solution for a coupled, discrete fracture continuum model. *Water Resources Research* 1983; **19**:959–969.
3. Savitski AA, Detournay E. Propagation of a penny-shaped fluid-driven fracture in an impermeable rock: asymptotic solutions. *International Journal of Solids and Structures* 2002; **39**:6311–6337.
4. Strack ODL. Flow in aquifers with clay laminae 1. The comprehensive potential. *Water Resources Research* 1981; **17**:985–992.
5. Gray LJ. Boundary element method for regions with thin internal cavities. *Engineering Analysis with Boundary Elements* 1989; **6**:180–184.
6. Gray LJ, Giles GE, Wendel MW. Boundary element method for regions with thin internal cavities. II. *Engineering Analysis with Boundary Elements* 1991; **6**:81–88.
7. Suresh S, Mortensen A. *Fundamentals of Functionally Graded Materials*. The Institute of Materials, IOM Communications Ltd.: London, 1998.
8. Miyamoto Y, Kaysser WA, Rabin BH, Kawasaki A, Ford RG. *Functionally Graded Materials*: *Design*, *Processing and Applications*. Kluwer Academic Publishers: Dordrecht, 1999.
9. Special issue: papers from the German Priority Programme (functionally graded materials). *Materials Science and Engineering A* 2003; **362**:1–331.
10. Paulino GH, Jin ZH, Dodds RH. Failure of functionally graded materials. In *Comprehensive Structural Integrity*, Karihaloo B, Knauss WG (eds), vol. 2, Chapter 13. Elsevier: Amsterdam, 2003; 607–644.
11. Bonnet M, Maier G, Polizzotto C. Symmetric Galerkin boundary element method. *Applied Mechanics Review* (ASME) 1998; **51**:669–704.
12. Gray LJ, San Soucie CA. Hermite interpolation algorithm for hypersingular boundary integrals. *International Journal for Numerical Methods in Engineering* 1993; **36**:2357–2367.
13. Gray LJ, Balakrishna C, Kane JH. Symmetric-Galerkin fracture analysis. *Engineering Analysis with Boundary Elements* 1995; **15**:103–109.
14. Paulino GH, Gray LJ. Galerkin residuals for error estimation and adaptivity in the symmetric Galerkin boundary integral method. *Engineering Mechanics* (ASCE) 1999; **125**:575–585.
15. Cheng AH-D. Darcy's flow with variable permeability: a boundary integral solution. *Water Resources Research* 1984; **20**:980–984.
16. Cheng AH-D. Heterogeneities in flows through porous media by the boundary element method. In *Topics in Boundary Element Research*, *Applications in Geomechanics*, Brebbia CA (ed.), vol. 4, Chapter 6. Springer: Berlin, 1987; 129–144.
17. Ingber MS, Phan-Thien N. A boundary element approach for parabolic equations using a class of particular solutions. *Applied Mathematical Modelling* 1992; **16**:124–132.
18. Ahmad S, Banerjee PK. Free vibration analysis of BEM using particular integrals. *Journal of Engineering Mechanics* 1986; **112**:682–695.
19. Partridge PW, Brebbia CA, Wrobel LC. *The Dual Reciprocity Boundary Element Method*. Computational Mechanics Publications: Southampton, Boston, 1992.
20. Nowak AJ. The multiple reciprocity method of solving transient heat conduction problems. In *BEM XI*, Brebbia CA, Connor JJ (eds). Computational Mechanics Publications, Springer: Southampton, Berlin, 1989; 81–95.
21. Power H. A complete multiple reciprocity approximation for the non-permanent stokes flow. In *Boundary Element Technology*, Brebbia CA, Kassab AJ (eds), vol. IX. Computational Mechanics Publications: Southampton, 1994; 127–137.

Copyright © 2005 John Wiley & Sons, Ltd.

22. Nardini D, Brebbia CA. A new approach to free vibration analysis using boundary elements. In *Boundary Element Methods in Engineering*, Brebbia CA (ed.). Springer: Berlin, 1982; 312–326.
23. Golberg MA, Chen CS. The method of fundamental solutions for potential, Helmholtz and diffusion problems. In *Boundary Integral Methods*: *Numerical and Mathematical Aspects*, Golberg MA (ed.). Computational Mechanics Publications: Southampton, 1999; 103–176.
24. Golberg MA, Chen CS, Bowman H, Power H. Some comments on the use of radial basis functions in the dual reciprocity method. *Computational Mechanics* 1998; **23**:141–148.
25. Ingber MS, Mammoli AA, Brown MJ. A comparison of domain integral evaluation techniques for boundary element methods. *International Journal for Numerical Methods in Engineering* 2001; **52**:417–432.
26. Sutradhar A, Paulino GH. A simple boundary element method for problems of potential in non-homogeneous media. *International Journal for Numerical Methods in Engineering* 2004; **60**:2203–2230.
27. Sutradhar A, Paulino GH. The simple boundary element method for transient heat conduction in functionally graded materials. *Computer Methods in Applied Mechanics and Engineering* 2004; **193**:4511–4539.
28. Ang WT, Kusuma J, Clements DJ. A boundary element method for a second order elliptic partial differential equation with variable coefficients. *Engineering Analysis with Boundary Elements* 1996; **18**:311–316.
29. Shaw RP, Makris N. Green's functions for Helmholtz and Laplace equations in heterogeneous media. *Engineering Analysis with Boundary Elements* 1992; **10**:179–183.
30. Shaw RP. Green's functions for heterogeneous media potential problems. *Engineering Analysis with Boundary Elements* 1994; **13**:219–221.
31. Harrouni KE, Quazar D, Wrobel LC, Brebbia CA. Dual reciprocity boundary element method for heterogeneous porous media. In *Boundary Element Technology VII*, Brebbia CA, Ingber MS (eds). Computational Mechanics Publication, Elsevier Applied Science: Southampton, Amsterdam, 1992; 151–159.
32. Harrouni KE, Quazar D, Wrobel LC, Cheng AH-D. Global interpolation function based DRBEM applied to Darcy's flow in heterogenous media. *Engineering Analysis with Boundary Elements* 1995; **16**:281–285.
33. Divo EA, Kassab AJ. *Boundary Element Method for Heat Conduction*: *With Applications in Non-Homogeneous Media*, Topics in Engineering Series, vol. 44. WIT Press: Billerica, MA, 2002.
34. Divo EA, Kassab AJ. Generalized boundary integral equation for heat conduction in non-homogeneous media: recent developments on the shifting property. *Engineering Analysis with Boundary Elements* 1998; **22**:221–234.
35. Bansal Y, Pindera MJ. Efficient reformulation of HOTFGM: heat conduction with variable thermal conductivity. *NASA CR 211910*, NASA-Glenn Research Center, Cleveland, OH, 2002.
36. Gray LJ, Kaplan T, Richardson JD, Paulino GH. Green's functions and boundary integral analysis for exponentially graded materials: heat conduction. *Journal of Applied Mechanics* (ASME) 2003; **70**:543–549.
37. Dumont NA, Chaves RAP, Paulino GH. The hybrid boundary element method applied to functionally graded materials. In *Boundary Elements XXIV*, Series: Advances in Boundary Elements, Brebbia CA, Tadeu A, Popov V (eds), vol. 13. Computational Mechanics Publication: Southampton, 2002; 267–276.
38. Sutradhar A, Paulino GH, Gray LJ. On hypersingular surface integrals in the symmetric Galerkin boundary element method: application to heat conduction in exponentially graded materials. *International Journal for Numerical Methods in Engineering* 2005; **62**:122–157.
39. Tanaka M, Matsumoto T, Suda Y. A dual reciprocity boundary element method applied to the steady-state heat conduction problem of functionally gradient materials. *Electronic Journal of Boundary Elements* 2002; **1**:128–135.
40. Kellogg OD. *Foundations of Potential Theory*. Dover: New York, 1953.
41. Georghitza SI. On the plane steady flow of water through inhomogeneous porous media. *The First International Symposium on the Fundamentals of Transport Phenomena in Porous Media*. International Association for Hydraulics Research: Israel, 1969.
42. Konda N, Erdogan F. The mixed mode crack problem in a non-homogeneous elastic medium. *Engineering Fracture Mechanics* 1994; **47**:533–545.
43. Gastaldi D. Microstructure-based numerical modelling of functionally graded materials for applications in the biomedical field. *Ph.D. Dissertation*, Politecnico di Milano, 2005.
44. Portela A, Aliabadi MH, Rooke DP. The dual boundary element method: efficient implementation for cracked problems. *International Journal for Numerical Methods in Engineering* 1992; **33**:1269–1287.
45. Mi Y, Aliabadi MH. Dual boundary element method for three-dimensional fracture mechanics analysis. *Engineering Analysis with Boundary Elements* 1992; **10**:161–171.
46. Crouch SL. Solution of plane elasticity problems by the displacement discontinuity method. *International Journal for Numerical Methods in Engineering* 1976; **10**:135–153.

Copyright © 2005 John Wiley & Sons, Ltd.

47. Crouch SL, Starfield AM. *Boundary Element Methods in Solid Mechanics*. George Allen and Unwin Ltd.: London, 1983.
48. Bonnet M. *Boundary Integral Equation Methods for Solids and Fluids*. Wiley: England, 1995.
49. Gray LJ, Glaeser J, Kaplan T. Direct evaluation of hypersingular Galerkin surface integrals. *SIAM Journal on Scientific Computing* 2002; **25**:1534–1556.
50. Gray LJ, Lutz ED. On the treatment of corners in the boundary element method. *Journal of Computational and Applied Mathematics* 1990; **32**:369–386.
51. *ABAQUS Version 6.2*. Hibbitt, Karlsson and Sorensen, Inc.: Pawtucket, RI, U.S.A., 2002.
52. Brebbia CA, Dominguez J. *Boundary Elements*: *An Introductory Course*. WIT Press: Boston, Southampton, 1992.
53. Berger JR, Martin PA, Mantic V, Gray LJ. Fundamental solutions for steady-state heat transfer in an exponentially-graded anisotropic material. *Zeitschrift für Angewandte Mathematik und Physik* 2005; **56**:293–303.
54. Clements DL, Budhi WS. A boundary element method of the solution of a class of steady-state problems for anisotropic media. *Journal of Heat Transfer* 1999; **19**:462–465.

Copyright © 2005 John Wiley & Sons, Ltd.